

# Unconventional pairing in few-fermion systems tuned by external confinement

Jacek Dobrzyniecki,<sup>1,\*</sup> Giuliano Orso,<sup>2</sup> and Tomasz Sowiński<sup>1</sup>

<sup>1</sup>*Institute of Physics, Polish Academy of Sciences, Aleja Lotników 32/46, PL-02668 Warsaw, Poland*

<sup>2</sup>*Université de Paris, Laboratoire Matériaux et Phénomènes Quantiques, CNRS, F-75013, Paris, France*

(Dated: March 26, 2022)

We study the ground-state properties of a two-component quasi-one-dimensional system of few ultra-cold fermions with attractive interactions. We show that, by ramping an external potential barrier felt by one of the components, it is possible to induce exotic superconducting phases characterized by a tunable finite net momentum of the Cooper pair, without changing the overall spin populations. We show that the pairing mechanisms can be distinguished by analyzing a specific two-particle correlation encoded in the noise correlation function. Our theoretical results can be addressed in current experiments with cold atoms confined in spin-selective optical traps.

## I. INTRODUCTION

Ultra-cold atoms provide an exceptional experimental platform to simulate condensed matter systems in a controlled way [1, 2]. One of the most spectacular collective phenomena in solids is superconductivity, where electrons with opposite spin and momenta bind into Cooper pairs, due to an effective attractive interaction mediated by the crystal vibrations. In the presence of a mismatch between the two spin populations, generated for instance by an applied Zeeman field, the conventional Bardeen–Cooper–Schrieffer (BCS) pairing mechanism becomes unstable, as some electrons will inevitably end up without partners. The spin-imbalanced system can nevertheless remain superconducting, at the price of adopting a new pairing mechanism harnessing the excess fermions. A well known example of superconductivity coexisting with a partial spin polarization is the Fulde–Ferrell–Larkin–Ovchinnikov (FFLO) state [3, 4], where Cooper pairs condense at a finite momentum. This implies that the associated order parameter becomes spatially modulated, with the excess fermions sitting at the nodes of the wave, where they are less detrimental to superconductivity.

The modulated phase is currently investigated in different physical systems, including one- and two-dimensional organic superconductors [5], hybrid structures [6] and quark-gluon plasma [7]. Over the last decade atomic Fermi gases have also emerged as a valid alternative to study this exotic state of matter (for a recent review see [8–10]) for a number of reasons: i) the two spin states correspond to two hyperfine levels, whose populations are fixed at the beginning of the experiment via a radio-frequency field, without generating vortices; ii) there is no disorder; iii) fermions can be confined in low-dimensional geometries, where the FFLO state is more robust. In particular, the ground state of one-dimensional (1D) systems with attractive contact interactions is known both theoretically [11–13] and numerically [14–17] to be of the FFLO type, for any finite value of the spin imbalance. The phase diagram of a

spin-imbalanced attractive 1D Fermi gas in a harmonic trap has been predicted in [18, 19] and experimentally verified in Ref. [20]. In particular the density profiles of the two spin components develop a two-shell structure, with the central part being a FFLO phase, while the wings are either fully paired or fully polarized, depending on the overall spin polarization. These predictions were also confirmed by DMRG studies of the Fermi Hubbard model [21]. To date, obtaining direct experimental evidence of the modulated phase with cold atoms is still challenging. Several detection schemes have been discussed, based on the analysis of collective oscillations [22], the sudden expansion of the gas [23–25], interaction quenches [26], noise correlations [27, 28], spectroscopy measurements [29–32] and the coupling to a Bose gas [33].

An interesting problem is to investigate the FFLO pairing in 1D Fermi gases in the presence of spin-dependent external potentials, so that the effective Zeeman field  $h$ , corresponding to the semi-difference between the local chemical potentials of the two spin components, is no longer uniform throughout the atomic cloud. A natural question then arises: can one tune the external confinement to induce different superconducting phases in the Fermi gas, *without* changing the overall spin populations? To answer this intriguing question, in this paper we investigate theoretically a 1D spin-1/2 system of a few attractively interacting fermions, confined in a box trap with an additional spin-dependent potential barrier at the trap center. Our main object of interest are the pairing correlations present in this system, which can be analyzed by means of the noise correlation distribution. Depending on the *local* population imbalance, the system behaves either as a BCS superconductor or a FFLO state, distinguishable by a nonzero center-of-mass-momentum of Cooper pairs. We show that by appropriately tuning the height and width of the potential barrier, it is possible to switch the system between different pairing types, even though the atom numbers of both components remain unchanged.

This work is organized as follows. In Sec. II, we describe the model system under study. In Sec. III we examine the pair correlations that arise in the box trap, without the potential barrier, and show how they can be

\* [Jacek.Dobrzyniecki@ifpan.edu.pl](mailto:Jacek.Dobrzyniecki@ifpan.edu.pl)

analyzed through noise correlation distributions. In Sec. IV, we describe the effect of the potential barrier, showing how the dominant net pair momentum changes as the barrier parameters (height and width) are modified. In Sec. V, we describe the particular case where the component split by the potential barrier has an odd number of fermions. Sec. VI contains the conclusions.

## II. THE MODEL

In this work we consider a one-dimensional system of a few fermions of mass  $m$  in two different internal states  $\sigma \in \{A, B\}$ , playing the role of effective spins. Motivated by state-of-the-art experiments with ultra-cold atoms in two hyperfine levels, we assume that the particle numbers  $N_A$  and  $N_B$  of the two spin components are fixed integers. The system is described by a second-quantized Hamiltonian of the form

$$\hat{\mathcal{H}} = \sum_{\sigma} \int dx \hat{\Psi}_{\sigma}^{\dagger}(x) \left( -\frac{\hbar^2}{2m} \frac{d^2}{dx^2} + \mathcal{V}_{\sigma}(x) \right) \hat{\Psi}_{\sigma}(x) + g \int dx \hat{n}_A(x) \hat{n}_B(x), \quad (1)$$

where the fermionic field operator  $\hat{\Psi}_{\sigma}(x)$  annihilates a  $\sigma$ -fermion at position  $x$  and obeys the conventional fermionic anticommutation relations,  $\{\hat{\Psi}_{\sigma}(x), \hat{\Psi}_{\sigma'}(x')\} = 0$  and  $\{\hat{\Psi}_{\sigma}(x), \hat{\Psi}_{\sigma'}^{\dagger}(x')\} = \delta_{\sigma\sigma'} \delta(x - x')$ . For convenience, we introduced the single-particle density operators  $\hat{n}_{\sigma}(x) = \hat{\Psi}_{\sigma}^{\dagger}(x) \hat{\Psi}_{\sigma}(x)$ . In the following we take the external potential  $\mathcal{V}_{\sigma}(x)$  as

$$\mathcal{V}_{\sigma}(x) = \begin{cases} V_{\sigma}, & |x| \leq D, \\ 0, & D < |x| \leq L, \\ \infty, & L < |x|, \end{cases} \quad (2)$$

with  $V_A = V$  and  $V_B = 0$ , respectively. It means that the particles are confined in an infinite square well of length  $2L$ , and the component  $A$  additionally feels a potential barrier of width  $2D$  and height  $V$  in the center of the box. From an experimental point of view, a spin-dependent external potential can be achieved *e.g.* by using a focused laser beam or magnetic field gradient to induce a spatially localized spin-selective energy shift [34–37].

The inter-particle interactions are modelled as contact interactions between fermions of opposite species with strength  $g$ . The interaction strength  $g$  is related to the three-dimensional  $s$ -wave scattering length [38, 39] and can be tuned by magnetic Feshbach resonances [40, 41] or by adjusting the confinement in a perpendicular direction [38].

For convenience, throughout the rest of this paper we employ dimensionless units, *i.e.*, we express all energies, lengths, and momenta in units of  $\hbar^2/mL^2$ ,  $L$ , and  $\hbar/L$ , respectively. In these units the interaction strength is expressed in units of  $\hbar^2/mL$ . Without losing the generality of the final conclusions, throughout this paper we set the strength of attractive interactions to  $g = -5$ .

To numerically obtain the many-body ground state for the given number of particles and external potential configuration, we first solve corresponding single-particle eigenproblems for each component separately. Then, we use the lowest-energy eigenorbitals to construct the non-interacting many-body Fock basis  $\{|F_i\rangle\}$ . Specifically, each Fock state  $|F_i\rangle$  is a product of two Slater determinants of  $N_A$  and  $N_B$  orbitals, describing the many-body state of  $A$  and  $B$  component, respectively. Since the many-body basis grows exponentially with the number of particles, we limit the basis to Fock states which have a non-interacting energy below a properly chosen value  $E_{\max}$ , according to the recipe given in [42]. Then the many-body Hamiltonian (1) is expressed as a matrix in the basis  $\{|F_i\rangle\}$  and diagonalized using the implicitly restarted Arnoldi method [43]. In this way, the ground state  $|G\rangle$  is found as its decomposition in the basis  $\{|F_i\rangle\}$  and used for further calculations. In the end, we confirm that the obtained results do not change quantitatively upon increase of the cutoff energy  $E_{\max}$ .

## III. PAIRING IN THE TRAPPED SYSTEM

For the attractive inter-component interactions ( $g < 0$ ), fermions of opposite species form strongly correlated pairs. It has been shown that these pairs may display many different features of the Cooper pairs known from the theory of superconductivity [44–48]. Identifying the type of pairing that arises (*i.e.* pairing with zero or nonzero net pair momentum) requires a detailed knowledge of the superconducting correlation function. It has been previously shown [27, 28, 49] that such information can also be obtained from the two-point noise correlation  $\mathcal{G}$  between the two components, which is directly experimentally accessible from two-body density measurements [50–52]. In the momentum domain, the distribution of the noise correlation is given by

$$\mathcal{G}(p_A, p_B) = \langle \hat{\pi}_A(p_A) \hat{\pi}_B(p_B) \rangle - \langle \hat{\pi}_A(p_A) \rangle \langle \hat{\pi}_B(p_B) \rangle, \quad (3)$$

where the momentum density operators  $\hat{\pi}_{\sigma}(p) = \hat{\Psi}_{\sigma}^{\dagger}(p) \hat{\Psi}_{\sigma}(p)$  are expressed straightforwardly in terms of Fourier-transformed field operators  $\hat{\Psi}_{\sigma}(p) = \int dx \hat{\Psi}_{\sigma}(x) \exp(-ipx/\hbar)$ . The noise correlation is the difference between the two-particle density distribution, and the product of individual single-particle densities. For a non-interacting system,  $\mathcal{G}(p_A, p_B)$  is zero everywhere. It means that  $\mathcal{G}(p_A, p_B)$  expresses the distribution of correlations forced by inter-particle interactions that cannot be captured by a single-particle description, excluding the spurious correlations that arise from single-particle densities.

To demonstrate that different types of correlated pairs are well-captured by the noise correlations, in Fig. 1 we show the distribution  $\mathcal{G}(p_A, p_B)$  in the absence of the potential barrier ( $V = 0$ ) and different imbalances  $\Delta N = N_B - N_A$ . For all balanced systems ( $\Delta N = 0$ ), an enhancement of inter-component correlations ( $\mathcal{G} > 0$ ) is

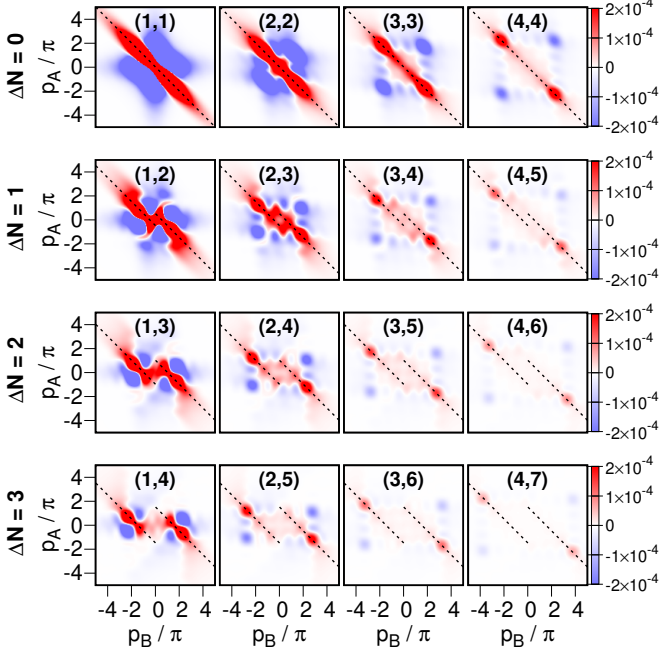


FIG. 1. The momentum noise correlation  $\mathcal{G}(p_A, p_B)$  in the ground state, calculated for systems with  $g = -5$ , potential barrier  $V = 0$ , and different particle numbers ( $N_A, N_B$ ). Each row includes systems with different imbalance  $\Delta N = N_B - N_A$ . For balanced systems ( $\Delta N = 0$ ), one sees an enhancement of correlations along the line  $p_A = -p_B$  (indicated by the dashed line), signalling BCS-like pairing of fermions with opposite momenta. For imbalanced systems, the enhanced correlations instead form along the lines  $p_A = -p_B \pm q_0$  (indicated by dashed lines), signalling the creation of FFLO-like pairs with net momentum  $\pm q_0$ . Momentum is given in units of  $\hbar/L$ , noise correlation in units of  $L^2/\hbar^2$ .

visible along the antidiagonal  $p_A = -p_B$ . It means that the probability of finding a pair of fermions with exactly opposite momenta is enhanced, which is a footprint of the standard Cooper-like pairing mechanism with zero pair momentum. For imbalanced systems ( $\Delta N > 0$ ), the situation is different. The region of enhanced correlations is split into two ridges, located along the two dashed lines, corresponding to net momenta  $p_A + p_B = \pm q_0$ , with  $q_0$  having a nonzero value, a hallmark of FFLO pairing.

The net FFLO pair momentum  $q_0$  in the box trap is expected to be equal to the difference  $\Delta p_F$  between the Fermi momenta  $p_{F\sigma} = N_\sigma \pi/2$  of the two spin components [53]

$$q_0 = \Delta p_F = \Delta N \pi/2. \quad (4)$$

Note that  $q_0$  depends only on the population imbalance  $\Delta N$  and not on the values  $N_A$  and  $N_B$  separately, unlike in non-uniform (e.g. harmonically trapped) systems [28]. The relation (4) is confirmed by Fig. 1 – for larger particle numbers, the noise correlation enhancement is concentrated into two clear, narrow maxima located at  $p_A \approx \pm N_A \pi/2, p_B \approx \mp N_B \pi/2$ . Separately, it is worth noting that the intensity of the noise correlations dimin-

ishes for higher particle numbers, because in 1D systems interactions effects are reduced as the particle density increases [18].

To identify the most probable net momentum  $q_0$  of the pair more clearly, we use a method previously proposed in [28]. It involves integrating the noise correlation with an appropriate filtering function  $\mathcal{F}(k)$ :

$$\mathcal{Q}(q) = \int dp_A dp_B \mathcal{F}(p_A + p_B - q) \mathcal{G}(p_A, p_B). \quad (5)$$

For the filtering function, we choose a simple Gaussian function  $\mathcal{F}(k) = (\pi w)^{-1/2} \exp(-k^2/2w^2)$ . The width parameter  $w = 0.5$  is of the order of the perpendicular width of the enhanced correlation area. We have checked that the form of  $\mathcal{Q}(q)$  is not significantly affected by small adjustments of  $w$ . Note that  $\mathcal{Q}(q) = \mathcal{Q}(-q)$ , due to the symmetry of  $\mathcal{G}$ . Therefore, for simplification, throughout the rest of this paper, we show its values only for positive  $q$ . In Fig. 2 we plot the function  $\mathcal{Q}(q)$  for systems with different particle numbers. The momentum  $q$  at which the function  $\mathcal{Q}$  takes its maximum value can be identified with the most likely net momentum  $q_0$  of the Cooper pairs in the system. Fig. 2a refers to systems with identical population imbalance  $\Delta N = 2$ , but varying particle numbers  $N_A$  and  $N_B$  (they correspond to the third row in Fig. 1). In all these cases, the maximum of  $\mathcal{Q}(q)$  falls at the same position  $q \simeq \pi$ , in agreement with the prediction (4). Conversely, in Fig. 2b we show  $\mathcal{Q}(q)$  for  $N_A = 2$  and different particle imbalances (corresponding to the second column in Fig. 1). The balanced system ( $\Delta N = 0$ ) with BCS pairing is characterized by a clear maximum at  $q \simeq 0$ . As the particle imbalance increases, the maximum occurs at increasingly higher momenta, in each case very close to the predicted value (4), indicated by the vertical dashed lines. This point is further illustrated in the inset in Fig. 2, showing the most likely pair momentum  $q_0$ , defined through the function  $\mathcal{Q}(q)$ , versus the Fermi momentum mismatch  $\Delta p_F$ , for various particle numbers and imbalances (see Table I for the exact numerical data). All data points fall very close to the dashed straight line, corresponding to  $q_0 = \Delta p_F$ , confirming that the the most likely net momentum of the Cooper pairs basically coincides with the mismatch between the Fermi momenta across a wide variety of system sizes.

#### IV. ROLE OF THE INTERNAL BARRIER

So far we have assumed that both spin components feel the same external (flat box) potential. Let us now consider the effects of changing the barrier height  $V$  felt solely by the component  $A$ . As  $V$  increases, the  $A$ -fermions are progressively pushed towards the lateral wings until the central region is completely emptied. In the high-barrier limit, the  $A$ -fermions effectively experience a symmetrical double-well potential with negligible tunneling between the two wells. Since each separate well

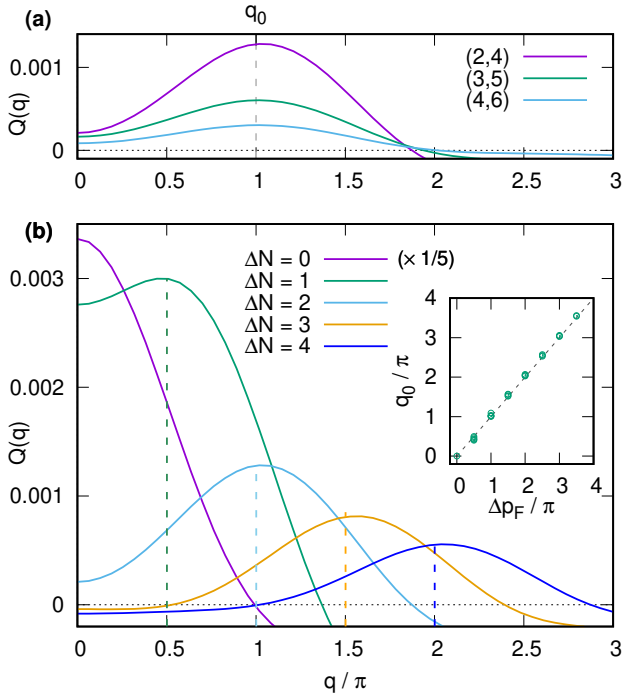


FIG. 2. (a) The function  $Q(q)$ , whose maxima indicate the most probable values of correlated pair momentum  $q_0$ , for few-body systems with fixed particle imbalance  $\Delta N = 2$  and different particle numbers ( $N_A, N_B$ ). The maximum in each case is present approximately at the value  $q = \pi$  (dashed line), equal to the Fermi momentum mismatch  $\Delta p_F$ . (b) The function  $Q(q)$  in systems with  $N_A = 2$  and different values of  $N_B = N_A + \Delta N$ . Note that the  $\Delta N = 0$  curve is scaled by  $1/5$ . Dashed lines indicate the theoretically predicted momenta  $\Delta N\pi/2$ . (Inset) The location of the maximum  $q_0$  in  $Q(q)$  (circles) as a function of the theoretically predicted Fermi momenta mismatch  $\Delta p_F$ . Different points correspond to different particle numbers and imbalances (see the numerical data in Table I for details). The dashed line corresponds to a theoretically predicted exact agreement  $q_0 = \Delta p_F$ . Momentum is given in units of  $\hbar/L$ ,  $Q(q)$  in units of  $L/\hbar$ .

has width  $1 - D$ , we see from (4) that the most likely net momentum  $q_0$  of Cooper pairs is given by

$$q_0 = \Delta N' \pi / (1 - D). \quad (6)$$

Here  $\Delta N' = N'_B - N'_A$ , where  $N'_\sigma$  is the number of fermions of component  $\sigma$  found within a given well. The latter can be determined by integrating the corresponding density profile  $n_\sigma(x) = \langle \hat{n}_\sigma(x) \rangle$  over the the well domain.

### A. Barrier with varying height

To demonstrate the effect of changing the barrier, let us consider a system with  $N_A = 4$  and  $N_B = 6$  fermions. In Fig. 3a, we examine its ground state properties for increasing  $V$ , assuming that the barrier width is fixed

$N_A$	$N_B$	$\Delta N$	$\Delta p_F/\pi$	$q_0/\pi$
1	2	1	0.5	0.50
2	3			0.47
3	4			0.44
4	5			0.42
5	6			0.40
1	3	2	1	1.09
2	4			1.03
3	5			1.02
4	6			1.01
5	7			1.01
1	4	3	1.5	1.57
2	5			1.56
3	6			1.53
4	7			1.52
1	5	4	2	2.07
2	6			2.05
3	7			2.04
4	8			2.03
1	6	5	2.5	2.57
2	7			2.55
3	8			2.53
1	7	6	3	3.06
2	8			3.04
3	9			3.03
1	8	7	3.5	3.56
2	9			3.54
1	9	8	4	4.06
2	10			4.04

TABLE I. The most probable net pair momentum  $q_0$  for systems with different particle numbers  $N_A, N_B$  and imbalances  $\Delta N = N_B - N_A$ . The system parameters are  $g = -5$  and  $V = 0$ . The pair momentum  $q_0$  is found as the location of the maximum of function  $Q(q)$ , defined in (5). It is compared to the theoretically predicted Fermi momentum difference  $\Delta p_F = \Delta N\pi/2$ . It is seen that  $q_0 \approx \Delta p_F$  in all cases, as predicted. Not shown are the entries for  $N_A = N_B$ , for which in all tested cases  $q_0 = \Delta p_F = 0$ .

to  $D = 1/3$ . We plot the single-particle densities  $n_A(x)$  and  $n_B(x)$ , along with the corresponding noise correlation distributions  $\mathcal{G}(p_A, p_B)$  and the function  $Q(q)$  that reflects the pair momentum distribution. In the homogeneous case ( $V = 0$ , top row in Fig. 3a), both densities (left column) are roughly evenly distributed throughout the box. Due to the population imbalance, the noise correlations in the system supports the FFLO-like pairing. The pair momentum calculated from (4) is  $q_0 = \pi$ , as seen from the locations of the positive maxima in  $\mathcal{G}$  (middle column).

As  $V$  increases, the component  $A$  is split and gradually pushed out from the center. Due to the symmetry of the system, the density  $n_A(x)$  is evenly split between the two side regions. Meanwhile, the density  $n_B(x)$  is es-

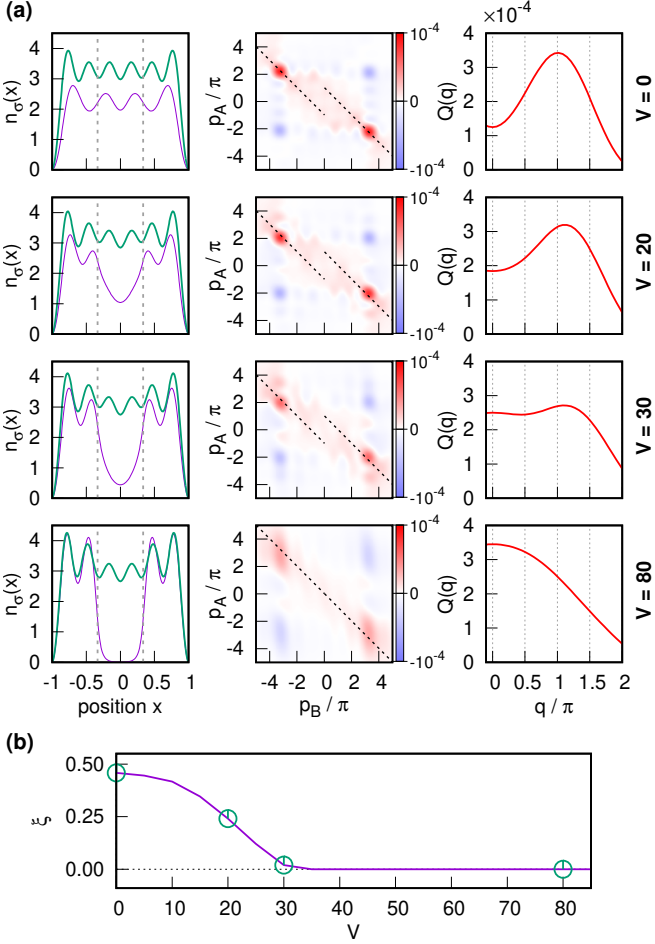


FIG. 3. The gradual transition of a system with FFLO-like pairing to BCS-like pairing as the potential barrier height  $V$  is tuned. The system parameters are  $N_A = 4$ ,  $N_B = 6$ ,  $g = -5$ ,  $D = 1/3$ . (a) Left column: The one-particle densities  $n_\sigma(x)$  in the ground state of the system for increasing  $V$ , for component  $A$  (thin lines) and  $B$  (thick lines). Dashed lines indicate the edges of the potential barrier  $-D \leq x \leq D$ . As  $V$  is increased, the  $A$ -component fermions are pushed out to the lateral regions, while the distribution of the  $B$ -fermions remains essentially unchanged. Middle column: Noise correlation distributions  $\mathcal{G}(p_A, p_B)$  of the system for increasing  $V$ . At  $V = 0$ , clear maxima are visible at  $p_A + p_B \approx \pi$ . For increasing  $V$  these maxima gradually vanish, replaced with more indistinct maxima close to the  $p_A = -p_B$  antidiagonal. Right column: The function  $\mathcal{Q}(q)$  for increasing  $V$ . At  $V = 0$  a clear maximum is present near  $q = \pi$ . For increasing  $V$ , the peak near  $q = \pi$  gradually vanishes while a maximum emerges at  $q = 0$ , indicating the switch from FFLO to BCS pairing. (b) The quantity  $\xi$ , defined in Eq. (7) and expressing the dominance of non-BCS pairing, as a function of  $V$ . Circles indicate the values of  $V$  depicted in the above plots. As  $V$  is increased and the BCS pairing becomes dominant,  $\xi$  decreases to zero. Energy is given in units of  $\hbar^2/mL^2$ ; position in units of  $L$ ; density  $n_\sigma$  in units of  $1/L$ ; momenta in units of  $\hbar/L$ ; noise correlation in units of  $L^2/\hbar^2$ ;  $\mathcal{Q}(q)$  in units of  $L/\hbar$ .

sentially unchanged (except for the slight modifications

due to the attractive interaction). The particular choice  $D = 1/3$  means that approximately one-third of the  $B$  population (two fermions) is located within each lateral region. As a result, for high  $V$ , the population within the lateral regions is balanced. This is additionally supported by the fact that densities  $n_A(x)$  and  $n_B(x)$  in these regions become almost identical. Thus, in this regime, the pairs created within the lateral regions are standard BCS Cooper-like pairs with zero net momentum. This is visible in the noise correlations – for the large  $V$  case (last row) the maxima are found close to the anti-diagonal  $p_A = -p_B$ . The maxima become gradually more indistinct and stretched along the  $p_A$  direction as  $V$  increases, which can be explained by the increasing uncertainty of  $p_A$  as the  $A$  fermions are squeezed into a smaller space.

The transition between FFLO and BCS pairing can be explained in greater detail by inspection of the function  $\mathcal{Q}(q)$  (right column in Fig. 3a). For  $V = 0$ ,  $\mathcal{Q}(q)$  displays a maximum at  $q_0 = \pi$ , exactly as predicted from the difference in Fermi momenta. As  $V$  increases, this maximum gradually vanishes, while simultaneously another maximum emerges at  $q_0 = 0$ . In particular, for  $V = 30$  one can distinguish two separate maxima at the two locations. This indicates that the change between the FFLO and BCS pairings is not a gradual decrease of  $q_0$ , but rather a direct switch between two distinct pairing mechanisms. A separate effect is that for small barrier heights  $V$ , the maximum at  $q_0 = \pi$  shifts towards slightly larger momenta, which can be explained by the fact that the momentum of  $A$ -fermions slightly increases due to the higher external potential energy.

From an experimental point of view, it is useful to define a measurable quantity that indicates whether the ground state of the system displays BCS or FFLO pairing. For this purpose, we define the dimensionless quantity

$$\xi = \frac{\int [\mathcal{Q}(q) - \mathcal{Q}(0)]\theta[\mathcal{Q}(q) - \mathcal{Q}(0)]dq}{\int \mathcal{Q}(q)\theta[\mathcal{Q}(q)]dq}, \quad (7)$$

where  $\theta(z)$  is the Heaviside step function. If the maximum of  $\mathcal{Q}(q)$  is located at  $q = 0$ ,  $\xi$  is exactly zero, while if the maximum falls at any other position then  $\xi > 0$ . The value of  $\xi$  can therefore be interpreted as an indicator for FFLO pairing. In Fig. 3b we show the value of  $\xi$  for the  $N_A = 4$ ,  $N_B = 6$  system as a function of  $V$ . As  $V$  increases,  $\xi$  gradually diminishes and eventually vanishes around  $V \simeq 35$ , signaling the transition towards the standard BCS pairing.

## B. Tuning the barrier width

The FFLO pair momentum  $q_0$  can also be controlled by tuning the width of the barrier. To demonstrate this, in Fig. 4a we show results for a system with  $N_A = 4$ ,  $N_B = 9$  particles obtained by progressively increasing the barrier width  $D$ , assuming a fixed barrier height  $V = 150$ . The

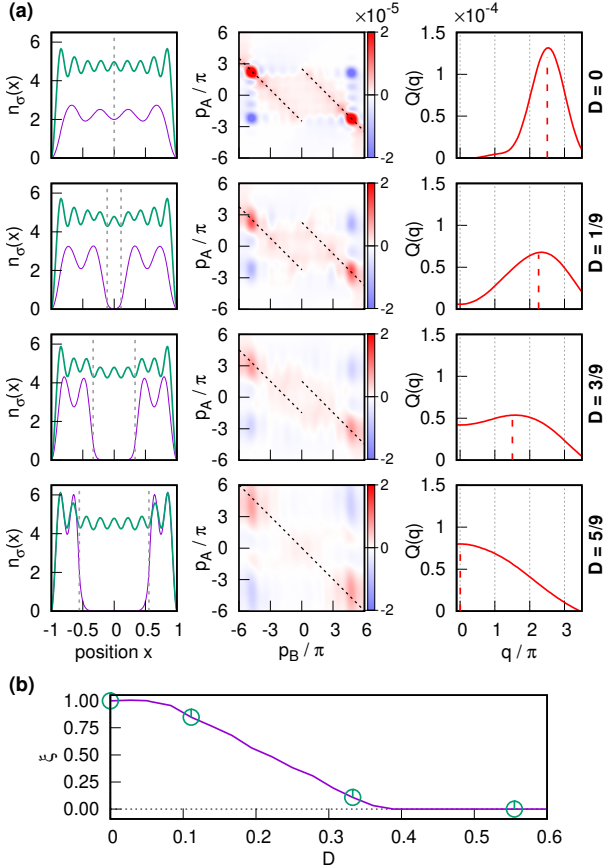


FIG. 4. The gradual change of the FFLO momentum as the barrier width parameter  $D$  is tuned. The system parameters are  $N_A = 4$ ,  $N_B = 9$ ,  $g = -5$ ,  $V = 150$ . (a) Left column: The one-particle densities  $n_\sigma(x)$  in the ground state of the system for increasing  $D$ . Dashed lines indicate the edges of the potential barrier  $-D \leq x \leq D$ . Middle column: Noise correlation distributions  $G(p_A, p_B)$  of the system for increasing  $D$ . As  $D$  increases, the maxima become gradually broader and more indistinct, owing to the increased uncertainty of momentum  $p_A$ . Right column: The function  $Q(q)$  for increasing  $V$ . Dashed lines indicate the predicted location of the preferred net momentum  $q_0$ , calculated from the difference of Fermi momenta. At  $D < 5/9$ , where the population of  $A$  and  $B$  in the lateral regions is unbalanced, the system exhibits a FFLO pairing with a changing net momentum. For  $D \approx 5/9$  the populations become balanced and the BCS pairing with  $q_0 = 0$  dominates instead. (b) Value of the quantity  $\xi$  as a function of  $D$ . Circles indicate the values of  $D$  depicted in the above plots. It is seen that the BCS pairing becomes dominant for  $D \gtrsim 0.4$ . Position and barrier width is given in units of  $L$ ; density  $n_\sigma$  in units of  $1/L$ ; momenta in units of  $\hbar/L$ ; noise correlation in units of  $L^2/\hbar^2$ ;  $Q(q)$  in units of  $L/\hbar$ .

latter choice ensures that the middle region is nearly empty of  $A$ -fermions. The single-particle densities  $n_\sigma(x)$  (left column in Fig. 4a) give an approximate view of the changing population difference in the lateral regions.

The first row shows the case of a system without a potential barrier. As seen from the noise correlation distri-

bution  $G(p_A, p_B)$  and the function  $Q(q)$  (middle and right column in Fig. 4a, respectively), in this case, FFLO-like pairs are formed with a nonzero momentum,  $q_0 = 5\pi/2$ . The subsequent rows show the effect of changing  $D$  to different values. The values of  $D = 1/9, 3/9, 5/9$  are chosen to ensure that the most probable value of  $N'_B$  is a clearly defined integer number (four, three, and two, respectively). Meanwhile,  $N'_A$  remains close to two in all cases. For each value of  $D$ , the noise correlation distribution and the function  $Q(q)$  show that the most probable pair momentum  $q_0$  changes to the value predicted from (6) indicated by vertical dashed lines ( $q_0 = 9\pi/4$ ,  $3\pi/2$ , and 0, respectively). These results clearly show that adjusting the barrier widths allows tuning the FFLO momentum  $q_0$ , as well as switching from FFLO pairing to BCS pairing. This point is further illustrated in Fig. 4b, showing the behavior of  $\xi$  as a function of  $D$ . In particular  $\xi$  decreases monotonically as  $D$  increases, and ultimately vanishes around  $D \simeq 0.4$ , marking the dominance of BCS pairing.

## V. ODD PARTICLE NUMBER

So far we have considered systems with an even particle number  $N_A$ . In those cases, the introduction of the potential barrier leads to an equal distribution of  $A$ -fermions in the two lateral regions. A more complicated situation occurs for systems with odd  $N_A$ . In this case, after the system is split into a double-well, the number of  $A$ -fermions in the two wells is no longer the same. As a consequence, the pair momentum  $q_0$  can take distinct values in the two lateral regions. To demonstrate this, we focus on the balanced case with  $N_A = N_B = 5$  particles. The single-particle densities, noise correlation and the function  $Q(q)$  for increasing values of  $V$  and fixed  $D = 1/5$  are shown in Fig. 5. For  $V = 0$ , the population of both components is exactly balanced and the system is characterized by BCS-like pairing with net pair momentum  $q_0 = 0$ . When  $V$  is increased, the density of the component  $A$  is split between the two wells. For very high  $V$  the most probable distribution is that of two  $A$ -fermions in one well, and three  $A$ -fermions in the other. It means that the one-body density  $n_A(x)$  within each well represents the contributions from density profiles corresponding to two or three fermions. Contrary, the expected number of  $B$ -fermions found in either of the wells is two, due to the chosen barrier width. Thus the imbalance  $\Delta N'$  is different in both wells, resulting in a dominance of two different values of net momentum,  $q_0 = 0$  and  $q_0 = 5\pi/4$ . This effect is indeed visible in the noise correlation  $G(p_A, p_B)$  and the function  $Q(q)$ , where distinct separate maxima are visible at the predicted values of  $q$ .

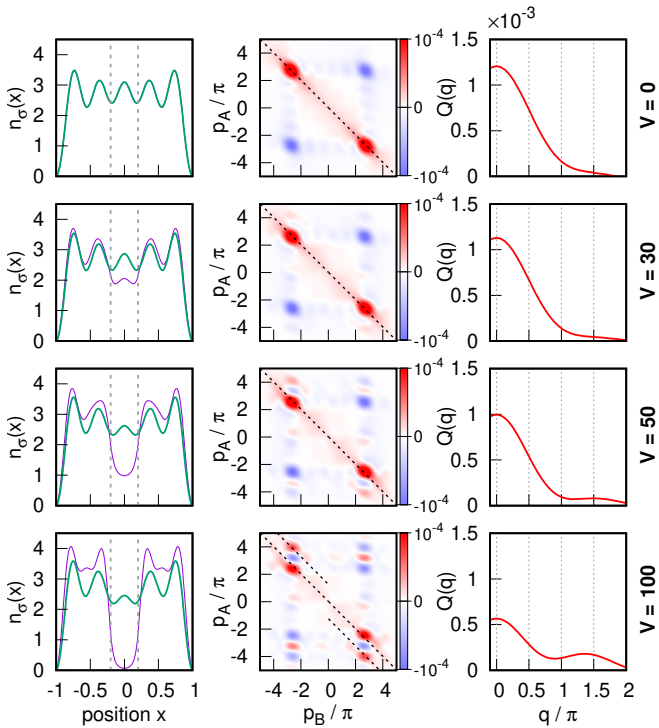


FIG. 5. The gradual change of a system with odd  $N_A$  as the potential barrier height  $V$  is tuned. The system parameters are  $N_A = 5, N_B = 5, g = -5, D = 1/5$ . (a) Left column: The one-particle densities  $n_\sigma(x)$  in the ground state of the system for increasing  $V$ . Dashed lines indicate the edges of the potential barrier  $-D \leq x \leq D$ . For  $V = 0$  the two densities are exactly identical. For a high potential barrier  $V$ , the  $A$  fermions are pushed out to the lateral regions. As the number of  $A$  fermions is odd, the density  $n_A(x)$  within each well represents the contributions from density profiles corresponding to two or three fermions. Middle column: Noise correlation distributions  $\mathcal{G}(p_A, p_B)$  of the system for increasing  $V$ . For a high barrier, two distinct maxima can be distinguished at  $p_1 + p_2 = 0$  and  $p_1 + p_2 = \pm 5\pi/4$ . Right column: The function  $Q(q)$  for increasing  $V$ . For a very high barrier, two maxima can be distinguished at  $q_0 = 0$  and  $q_0 = 5\pi/4$ . Energy is given in units of  $\hbar^2/mL^2$ ; position in units of  $L$ ; density  $n_\sigma$  in units of  $1/L$ ; momenta in units of  $\hbar/L$ ; noise correlation in units of  $L^2/\hbar^2$ ;  $Q(q)$  in units of  $L/\hbar$ .

## VI. CONCLUSION

Few-body cold atoms systems represent an intriguing platform to study pairing phenomena. Here we have investigated a one-dimensional system of few attractively interacting spin-1/2 fermions confined in a flat box trap, through the numerical study of the ground state density profiles and noise correlations. We show that by ramping up a central potential barrier felt by one of the two components, and thus restricting pair formation to regions outside the barrier, the system can undergo different pairing mechanisms without changing the overall spin populations. Specifically, solely by adjusting the barrier height and width, the particles can form either BCS-like pairs with zero center-of-mass momentum, or FFLO-like pairs with a tunable finite momentum.

In this work we have focused on the simplest case where only the confinement felt by one species is modified. It is possible to further extend the approach, for example by adjusting the barrier height for both components simultaneously. Our theoretical predictions can be addressed in state-of-the-art experiments with cold atoms. Relevant quantities such as density profiles and noise correlations can be directly measured and the spin dependent external potential can be tailored with current optical techniques.

## VII. ACKNOWLEDGMENTS

J.D. and T.S. acknowledge financial support from the (Polish) National Science Center (Grant No. 2016/22/E/ST2/00555). G. O. acknowledges financial support from ANR (Grant SpiFBox) and from DIM Sirteq (Grant EML 19002465 1DFG).

- 
- [1] Stefano Giorgini, Lev P. Pitaevskii, and Sandro Stringari, “Theory of ultracold atomic fermi gases,” *Rev. Mod. Phys.* **80**, 1215–1274 (2008).
- [2] I. Bloch, J. Dalibard, and W. Zwerger, “Many-body physics with ultracold gases,” *Rev. Mod. Phys.* **80**, 885–964 (2008).
- [3] Peter Fulde and Richard A. Ferrell, “Superconductivity in a strong spin-exchange field,” *Phys. Rev.* **135**, A550–A563 (1964).
- [4] A. I. Larkin and Y. N. Ovchinnikov, “Nonuniform state of superconductors,” *Zh. Eksp. Teor. Fiz.* **47**, 1136–1146 (1964), [Sov. Phys. JETP 20, 762(1965)].
- [5] G. Kourouklis, H. Kühne, J. A. Schlueter, J. Wosnitza, and S. E. Brown, “Microscopic study of the fulde-ferrell-larkin-ovchinnikov state in an all-organic superconductor,” *Phys. Rev. Lett.* **116**, 067003 (2016).
- [6] A. I. Buzdin, “Proximity effects in superconductor-ferromagnet heterostructures,” *Rev. Mod. Phys.* **77**, 935 (2005).
- [7] Roberto Casalbuoni and Giuseppe Nardulli, “Inhomogeneous superconductivity in condensed matter and QCD,” *Rev. Mod. Phys.* **76**, 263–320 (2004).
- [8] Frédéric Chevy and Christophe Mora, “Ultra-cold polarized fermi gases,” *Reports on Progress in Physics* **73**,

- 112401 (2010).
- [9] A. E. Feiguin, F. Heidrich-Meisner, G. Orso, and W. Zwerger, “Bcs–bec crossover and unconventional superfluid order in one dimension,” in *The BCS-BEC Crossover and the Unitary Fermi Gas* (Springer, 2012) pp. 503–532.
- [10] Jami J. Kinnunen, Jildou E. Baarsma, Jani-Petri Martikainen, and Päivi Törmä, “The fulde–ferrell–larkin–ovchinnikov state for ultracold fermions in lattice and harmonic potentials: a review,” *Rep. Prog. Phys.* **81**, 046401 (2018).
- [11] Kun Yang, “Inhomogeneous superconducting state in quasi-one-dimensional systems,” *Phys. Rev. B* **63**, 140511 (2001).
- [12] Xi-Wen Guan, Murray T. Batchelor, and Chaohong Lee, “Fermi gases in one dimension: From bethe ansatz to experiments,” *Rev. Mod. Phys.* **85**, 1633–1691 (2013).
- [13] Song Cheng, Yi-Cong Yu, M. T. Batchelor, and Xi-Wen Guan, “Fulde–ferrell–larkin–ovchinnikov correlation and free fluids in the one-dimensional attractive hubbard model,” *Phys. Rev. B* **97**, 121111(R) (2018).
- [14] A. E. Feiguin and F. Heidrich-Meisner, “Pairing states of a polarized fermi gas trapped in a one-dimensional optical lattice,” *Phys. Rev. B* **76**, 220508(R) (2007).
- [15] G. G. Batrouni, M. H. Huntley, V. G. Rousseau, and R. T. Scalettar, “Exact numerical study of pair formation with imbalanced fermion populations,” *Phys. Rev. Lett.* **100**, 116405 (2008).
- [16] Masaki Tezuka and Masahito Ueda, “Density-matrix renormalization group study of trapped imbalanced fermi condensates,” *Phys. Rev. Lett.* **100**, 110403 (2008).
- [17] Michele Casula, D. M. Ceperley, and Erich J. Mueller, “Quantum monte carlo study of one-dimensional trapped fermions with attractive contact interactions,” *Phys. Rev. A* **78**, 033607 (2008).
- [18] G. Orso, “Attractive fermi gases with unequal spin populations in highly elongated traps,” *Phys. Rev. Lett.* **98**, 070402 (2007).
- [19] Hui Hu, Xia-Ji Liu, and Peter D. Drummond, “Phase diagram of a strongly interacting polarized fermi gas in one dimension,” *Phys. Rev. Lett.* **98**, 070403 (2007).
- [20] Yean-an Liao, Ann Sophie C. Rittner, Tobias Paprota, Wenhui Li, Guthrie B. Partridge, Randall G. Hulet, Stefan K. Baur, and Erich J. Mueller, “Spin-imbalance in a one-dimensional Fermi gas,” *Nature* **467**, 567 (2010).
- [21] F. Heidrich-Meisner, G. Orso, and A. E. Feiguin, “Phase separation of trapped spin-imbalanced fermi gases in one-dimensional optical lattices,” *Phys. Rev. A* **81**, 053602 (2010).
- [22] Jonathan M. Edge and N. R. Cooper, “Signature of the fulde–ferrell–larkin–ovchinnikov phase in the collective modes of a trapped ultracold fermi gas,” *Phys. Rev. Lett.* **103**, 065301 (2009).
- [23] J. Kajala, F. Massel, and P. Törmä, “Expansion dynamics of the fulde–ferrell–larkin–ovchinnikov state,” *Phys. Rev. A* **84**, 041601(R) (2011).
- [24] H. Lu, L. O. Baksmaty, C. J. Bolech, and H. Pu, “Expansion of 1d polarized superfluids: The fflo state reveals itself,” *Phys. Rev. Lett.* **108**, 225302 (2012).
- [25] C. J. Bolech, F. Heidrich-Meisner, S. Langer, I. P. McCulloch, G. Orso, and M. Rigol, “Long-time behavior of the momentum distribution during the sudden expansion of a spin-imbalanced fermi gas in one dimension,” *Phys. Rev. Lett.* **109**, 110602 (2012).
- [26] L. Riegger, G. Orso, and F. Heidrich-Meisner, “Interaction quantum quenches in the one-dimensional fermi-hubbard model with spin imbalance,” *Phys. Rev. A* **91**, 043623 (2015).
- [27] Andreas Lüscher, Reinhard M. Noack, and Andreas M. Läuchli, “Fulde-ferrell-larkin-ovchinnikov state in the one-dimensional attractive hubbard model and its fingerprint in spatial noise correlations,” *Phys. Rev. A* **78**, 013637 (2008).
- [28] Daniel Pęcak and Tomasz Sowiński, “Signatures of unconventional pairing in spin-imbalanced one-dimensional few-fermion systems,” *Phys. Rev. Research* **2**, 012077 (2020).
- [29] Anna Korolyuk, Francesco Massel, and Päivi Törmä, “Probing the fulde–ferrell–larkin–ovchinnikov phase by double occupancy modulation spectroscopy,” *Phys. Rev. Lett.* **104**, 236402 (2010).
- [30] M. Reza Bakhtiari, M. J. Leskinen, and P. Törmä, “Spectral signatures of the fulde–ferrell–larkin–ovchinnikov order parameter in one-dimensional optical lattices,” *Phys. Rev. Lett.* **101**, 120404 (2008).
- [31] T. Roscilde, M. Rodríguez, K. Eckert, O. Romero-Isart, M. Lewenstein, E. Polzik, and A. Sanpera, “Quantum polarization spectroscopy of correlations in attractive fermionic gases,” *New J. Phys.* **11**, 055041 (2009).
- [32] Roman M. Lutchyn, Maxim Dzero, and Victor M. Yakovenko, “Spectroscopy of the soliton lattice formation in quasi-one-dimensional fermionic superfluids with population imbalance,” *Phys. Rev. A* **84**, 033609 (2011).
- [33] Manpreet Singh and Giuliano Orso, “Enhanced visibility of the fulde–ferrell–larkin–ovchinnikov state in one-dimensional bose-fermi mixtures near the immiscibility point,” *Phys. Rev. Research* **2**, 023148 (2020).
- [34] D. Schrader, I. Dotsenko, M. Khudaverdyan, Y. Mironchik, A. Rauschenbeutel, and D. Meschede, “Neutral atom quantum register,” *Phys. Rev. Lett.* **93**, 150501 (2004).
- [35] Chuanwei Zhang, S. L. Rolston, and S. Das Sarma, “Manipulation of single neutral atoms in optical lattices,” *Phys. Rev. A* **74**, 042316 (2006).
- [36] P. J. Lee, M. Anderlini, B. L. Brown, J. Sebby-Strabley, W. D. Phillips, and J. V. Porto, “Sublattice addressing and spin-dependent motion of atoms in a double-well lattice,” *Phys. Rev. Lett.* **99**, 020402 (2007).
- [37] Christof Weitenberg, Manuel Endres, Jacob F. Sherson, Marc Cheneau, Peter Schauß, Takeshi Fukuhara, Immanuel Bloch, and Stefan Kuhr, “Single-spin addressing in an atomic mott insulator,” *Nature* **471**, 319 (2011).
- [38] M. Olshanii, “Atomic scattering in the presence of an external confinement and a gas of impenetrable bosons,” *Phys. Rev. Lett.* **81**, 938 (1998).
- [39] E. Haller, M. Gustavsson, M. J. Mark, J. G. Danzl, R. Hart, G. Pupillo, and H.-C. Nägerl, “Realization of an excited, strongly correlated quantum gas phase,” *Science* **325**, 1224 (2009).
- [40] C. J. Pethick and H. Smith, *Bose-Einstein Condensation in Dilute Gases* (Cambridge University Press, 2008).
- [41] Cheng Chin, Rudolf Grimm, Paul Julienne, and Eite Tiesinga, “Feshbach resonances in ultracold gases,” *Rev. Mod. Phys.* **82**, 1225 (2010).
- [42] A. Chrostowski and T. Sowiński, “Efficient construction of many-body fock states having the lowest energies,” *Acta Phys. Polon. A* **136**, 566 (2019).

- [43] R. B. Lehoucq, D. C. Sorensen, and C. Yang, *Arpack User's Guide: Solution of Large-Scale Eigenvalue Problems with Implicitly Restarted Arnoldi Methods* (Society for Industrial and Applied Mathematics, 1998).
- [44] G. Zürn, A. N. Wenz, S. Murmann, A. Bergschneider, T. Lompe, and S. Jochim, “Pairing in few-fermion systems with attractive interactions,” *Phys. Rev. Lett.* **111**, 175302 (2013).
- [45] Pino D’Amico and Massimo Rontani, “Pairing of a few fermi atoms in one dimension,” *Phys. Rev. A* **91**, 043610 (2015).
- [46] Tomasz Sowiński, Mariusz Gajda, and Kazimierz Rzążewski, “Pairing in a system of a few attractive fermions in a harmonic trap,” *EPL* **109**, 26005 (2015).
- [47] Johannes Hofmann, Alejandro M. Lobos, and Victor Galitski, “Parity effect in a mesoscopic fermi gas,” *Phys. Rev. A* **93**, 061602 (2016).
- [48] Patrycja Łydźba and Tomasz Sowiński, “Unconventional pairing in one-dimensional systems of a few mass-imbalanced ultracold fermions,” *Phys. Rev. A* **101**, 033603 (2020).
- [49] Lukas Rammelmüller, Joaquín E. Drut, and Jens Braun, “Pairing patterns in one-dimensional spin- and mass-imbalanced Fermi gases,” *SciPost Phys.* **9**, 14 (2020).
- [50] Ehud Altman, Eugene Demler, and Mikhail D. Lukin, “Probing many-body states of ultracold atoms via noise correlations,” *Phys. Rev. A* **70**, 013603 (2004).
- [51] L. Mathey, E. Altman, and A. Vishwanath, “Noise correlations in one-dimensional systems of ultracold fermions,” *Phys. Rev. Lett.* **100**, 240401 (2008).
- [52] L. Mathey, A. Vishwanath, and E. Altman, “Noise correlations in low-dimensional systems of ultracold atoms,” *Phys. Rev. A* **79**, 013609 (2009).
- [53] We recall that in our units the system size is equal to 2.